Supporting Information

Passive targeting of high-grade gliomas via EPR effect: a closed path for metallic nanoparticles?

Carlos Caro1, Ashish Avasthi1, Jose M. Paez-Muñoz1, Manuel Pernía-Leal2,*, Maria L. García-Martín1,3,*

1 BIONAND – Centro Andaluz de Nanomedicina y Biotecnología (Junta de Andalucía-Universidad de Málaga), C/ Severo Ochoa, 35, 29590 Málaga, Spain.

2 Departamento de Química Orgánica y Farmacéutica, Facultad de Farmacia, Universidad de Sevilla, 41012 Sevilla, Spain

3 Biomedical Research Networking Center in Bioengineering, Biomaterials & Nanomedicine (CIBER-BBN)

*E-mails: mpernia@us.es; mlgarcia@bionand.es

Index

1. Methods

A) Synthesis of Iron Oleate

B) Synthesis of PEGylated ligand

C) Functionalization of MMNPs

D) Nuclear Magnetic Resonance Spectroscopy (NMR).

E) Fourier Transform Infra-Red Spectroscopy (FTIR)

F) Dynamic Light Scattering (DLS)

G) *In vitro* longitudinal and transversal relaxivities (r_1 and r_2)

H) Cytotoxicity assays

I) *In vivo* MRI experiments

J) Histology

2. Results

A) Characterization

B) *In vitro* transversal relaxivity.

C) Cytotoxicity assays

D) *In vivo* toxicity

1. Methods.

A) Synthesis of Iron oleate. Briefly, a mixture of 10.8 g of iron chloride (40 mmol) and 36.5 g of sodium oleate (120 mmol) were solved in 80 ml of ethanol, 60 ml of distilled water, and 140 ml of hexane. The resulting solution was heated up to 60°C and let for 4 h allowing reflux of hexane in an inert atmosphere. At that time, the reaction was cooled down to room temperature, and two phases could be distinguished: a lower aqueous phase and an upper organic phase containing the iron oleate. The organic phase was washed 3 times with distilled water, and the hexane was evaporated in the rotavapor.

B) Synthesis of PEGylated ligand

The gallol-PEGn-OH was synthesized following the previously synthetic route reported by us.[1, 2] In brief, to a solution of polyethylene glycol (Mw: 1500 g/mol or 3000 g/mol, 1.5 g or 3 g, 1 mmol for both cases), gallic acid (Mw: 170 g/mol, 1 mmol, 170 mg) and 4-(dimethylamino) pyridine (Mw: 122 g/mol, 200 μmol, 24 mg) in 100 mL of tetrahydrofuran and 10 mL of dichloromethane, in a round-bottom flask under nitrogen atmosphere, was added dropwise to a solution of dicyclohexyl carbodiimide (Mw: 206 g/mol, 5 mmol, 1 g) in toluene. The mixture was stirred overnight at room temperature. The reaction mixture was filtered through a filter paper and solvents were rota-evaporated. The crude product was dissolved in 100 mL of milli-Q water and the solution was adjusted to pH 2 by adding a few mL of a 0.1 mM HCl solution. The product was extracted from the water phase with dichloromethane (100 mL, three times). The organic layer was dried over Na_2SO_4, filtered through a filter paper and the solvent was rota-evaporated. 1H NMR spectroscopy confirmed the desired product gallol-PEG-OH. 1H NMR (400 MHz, $CDCl_3$) δ (ppm): 7.22 (s, 2H), 4.43-4.40 (m, 2H), 3.85-3.45 (m, CH_2-PEG, -OH). FTIR peaks (cm^{-1}): 1466 (C-H bend vibration), 1359 (C-H bend vibration), 1341 (C-H bend vibration), 1307 (anti-symmetric stretch vibration), 1268 (C-O stretch vibration), 1238 (C-O stretch vibration), 1092 (C-O-C stretch vibration), 942 (CH out-of-plane bending vibration).

C) Functionalization of MMNPs. Briefly, in a glass vial, a solution of 1.0 mL of nanoparticles (10 g/L of Fe), 1.0 mL of the gallol-PEGn-OH derived in a concentration of 0.1 M in $CHCl_3$ and 50 μL of triethylamine was added. The mixture was ultrasonicated for 1 h, and kept 4 h at 50ºC. At this point, it was diluted with 5 mL of toluene, 5 mL of milli-Q water and 10 mL of acetone. Then, it was shaken, and the nanoparticles were transferred into the aqueous phase. After that, the aqueous phase was collected in a round-bottom flask and the residual organic solvents were rota-evaporated. This mixture was shaken, prompting the transfer of the nanoparticles into the aqueous phase. Afterwards, this aqueous phase was collected in a round-bottom flask and the residual organic solvents were rota-evaporated. Then, the gallol derived MMNPs were purified

in centrifuge filters with a molecular weight cutoff of 100 kDa at 450 rcf. In each centrifugation, the functionalized MMNPs were re-suspended with milli-Q water. The purification step was repeated several times until the filtered solution was clear. After the purification, the gallol derived MMNPs were re-suspended in PBS buffer. Finally, to ensure high stable mono-dispersed magnetic nanoparticles, the solution was centrifuged at 150 rcf for 5 min and, it was placed onto a permanent magnet (0.6 T) for 5 min.

D) Nuclear Magnetic Resonance Spectroscopy (NMR). ^{1}H-NMR spectra of samples prepared in CDCl3 were recorded on a Bruker Ascend 400MHz NMR spectrometer.

E) Fourier Transform Infra-Red Spectroscopy (FTIR). FTIR spectra were recorded with an FTIR-4100 Jasco using a single reflection ATR accessory (MIRacle ATR, PIKE Technologies) coupled to a liquid nitrogen-cooled mercury cadmium telluride (MCT) detector. All spectra were recorded in the 4000 to 800 cm^{-1} range at 4 cm^{-1} resolution and accumulating 50 scans. Gallol derived ligands were deposited as solid products, and magnetic nanoparticles were prepared by dropcasting a highly concentrated nanoparticle solution onto a microscope slide (Thermo Scientific).

F) Dynamic Light Scattering (DLS). DLS measurements were done on a cell type ZEN0118-low volume disposable sizing cuvette, setting 2.420 as refractive index with 173º Backscatter (NIBS default) as angle of detection. The measurement duration was set as automatic and three as the number of measurements. As analysis model was chosen general purpose (normal resolution). To properly measure the DLS on FBS, we set the next values for the dispersant: 1.3568 as refractive index, 0.94 cP as viscosity and 80 as dielectric constant. For the size distribution measurement, the number mean was selected.

G) *In vitro* longitudinal and transversal relaxivities (r1 and r2). Regions of interest (ROIs) were drawn on the first image of the image sequence and the intensity values extracted and fit to the following equations:

$$M_Z(t) = M_0(1 - e^{-TR/T_1})$$

$$M_{XY}(t) = M_0 e^{-TE/T_2}$$

Where M_z and M_{xy} are the signal intensities at time TR or TE, and M_0 is the signal intensity at equilibrium.

H) Cytotoxicity assays.

MTT assay: Briefly, the N13 cells were plated at a density of $1x10^4$ cells/well in a 96-well plate at 37 ºC in 5 % CO_2 atmosphere (200 µL per well, number of repetitions = 5). After 24 h of culture, the medium in the wells was replaced with fresh medium containing SPIONs in varying concentrations from 0.1 µg/mL to 100 µg/mL. After 24 h, the supernatant of each well was replaced by 200 µL of fresh medium with 3-[4,5-dimethylthiazol-2-yl]-2,5-diphenyl tetrazolium

bromide (MTT) (0.5 mg/mL). After 2 h of incubation at 37 ºC and 5 % CO_2 the medium was removed and the formazan crystals were solubilized with 200 μL of DMSO, and the solution was vigorously mixed to dissolve the reacted dye. The absorbance of each well was read on a microplate reader (Dynatech MR7000 instruments) at 550 nm. The relative cell viability (%) and its error related to control wells containing cell culture medium without nanoparticles were calculated by the equations:

$$RCV(\%) = \left(\frac{[Abs]test - [Abs]Pos.Ctrl}{[Abs]Neg.Ctrl - [Abs]Pos.Ctrl}\right) \times 100$$

$$Error(\%) = \mathrm{RCVtest} \times \sqrt{\left(\frac{[\sigma]\mathrm{test}}{[\mathrm{Abs}]\mathrm{test}}\right)^2 + \left(\frac{[\sigma]\mathrm{control}}{[\mathrm{Abs}]\mathrm{control}}\right)^2}$$

where σ is the standard deviation. Triton X-100 was added to the positive control wells.

Cell morphology studies: The N13 cells were plated at a density of $1x10^4$ cells/well in a 96-well plate at 37 ºC in 5% CO_2 atmosphere (200 μL per well, number of repetitions = 5). After 24 h of culture, the medium in the wells was replaced with fresh medium containing the magnetic nanoparticles in varying concentrations from 0.1 μg/mL to 100 μg/mL. Similar to the cytotoxicity assays, after 24 h, the Triton X-100 was added to the positive control wells. After 15 min, all the wells were stained with DAPI (4',6-Diamidino-2-phenylindole) (dilution 1:3000) to label nuclei in all cells, although with stronger labeling in live cells, calcein (1:1000) to evaluate cell activity and TO-PRO-3 Iodine to only label dead cells (dilution 1:1000). The cell morphology images were acquired using a Perkin Elmer Operetta High Content Imaging System with a 20x LWD 0.45 NA air objective lens. 5 well replicas for each condition were analyzed with 10 random image fields captured per well. For each field, fluorescence images for DAPI, calcein, and TO-PRO-3, plus a brightfield image, were captured. Cell mortality percentages were calculated automatically by Operetta Harmony software, whereby all nuclei (dead and alive) were identified from the DAPI staining and the percentage of dead cells then determined by the number of nuclei also possessing high levels of TO-PRO-3 staining. Intracellular esterase activity was evaluated by calcein staining.

I) *In vivo* MRI experiment. MRI experiments were carried out on a 9.4 T Bruker Biospec system equipped with 400 mT/m gradients. An 86mm-inner-diameter volume resonator was used for excitation, and a surface coil designed for the rat head was used for signal reception. All the in vivo experiments were performed using the following experimental scheme: i) acquisition of high-resolution T_2-weighted images, ii) acquisition of T_2 parametric images (quantitative), iii) intravenous injection of the nanoparticles, iv) acquisition of a dynamic sequence of T_2-weighted images (pharmacokinetics time-courses), v) acquisition of high-resolution T_2-weighted images, vi) acquisition of T_2 parametric images (quantitative) and vii) acquisition of a dynamic sequence of T_1-weighted images (pharmacokinetics time-courses). High-resolution T_2-weighted images were acquired using a turbo-RARE sequence with respiratory gating (TE = 33 ms, TR = 2500 ms, 2 averages, 384 μm in-plane resolution and 1 mm slice thickness). Quantitative T_2 measurements were also performed using a multi-echo spin echo CPMG sequence (TEs ranging

from 7 ms to 224 ms, TR = 3000 ms, FOV = 32x32 mm, matrix size = 192x192, slice thickness = 1 mm). The T_2 time-courses were followed by using a turbo-RARE sequence with the same parameters indicated above, but only 1 average to improve temporal resolution (1 image every 30 seconds). The T_1 time-courses were followed by using a RARE sequence with respiratory gating (TE = 2.5 ms, TR = 27.778 ms, 1 averages, 192 μm in-plane resolution and 1 mm slice thickness).

J) Histology. The tissues were fixed in 4% formaldehyde (Panreac, pH 7 buffered) for 48 h, changing the 4% formaldehyde after 24 h. Then, the samples were dehydrated through graded ethanol and embedded in paraffin (temperature 56° C for 2 h under stirring and vacuum). The detailed procedures are described below.

Haematoxylin and Eosin (H&E): paraffin-embedded samples were sectioned at 7 μm thickness, then deparaffinized, rehydrated and stained with H&E, and then dehydrated in ascending concentrations of ethanol, cleared in xylene, and mounted on commercial glass slides.

Prussian Blue (PB): paraffin-embedded samples were sectioned at 7 μm thickness, then deparaffinized, rehydrated, submerged in 20% hydrochloric acid and 10% potassium ferrocyanide, washed with water and counterstained with Nuclear Fast Red, dehydrated in ascending concentrations of ethanol, cleared in xylene and mounted in commercial glass slides.

2. Results

A) Characterization

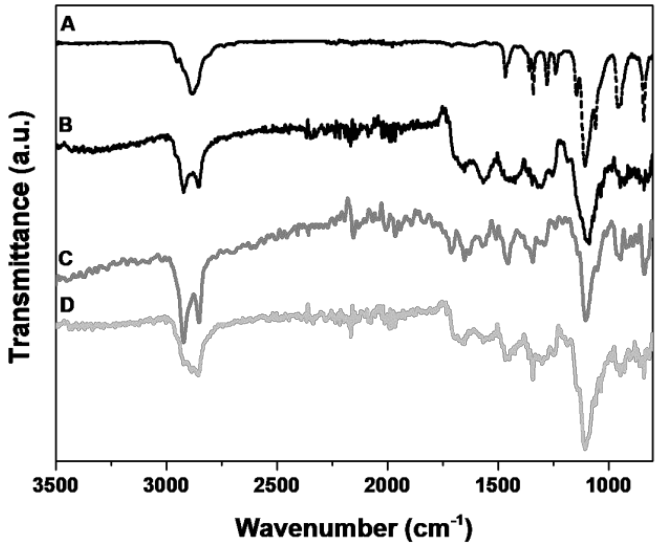

Figure S1. FTIR spectra of the free ligand (A), MMNP1 (B), MMNP2 (C) and MMNP3 (D).

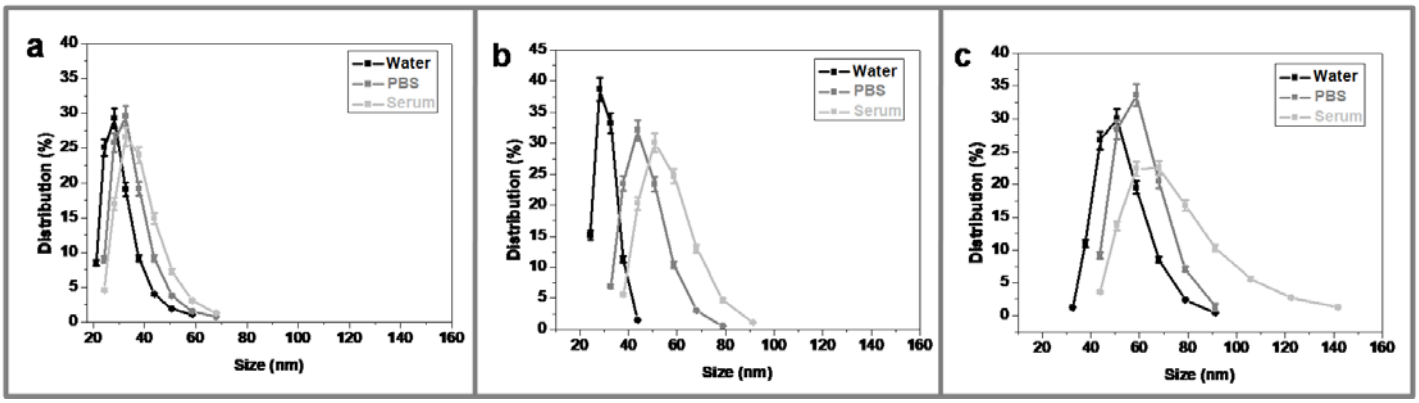

Figure S2. DLS spectra of MMNP1 (a), MMNP2 (b) and MMNP3 (c) in different dispersants: water (black lines), PBS (grey lines) and FBS (light grey lines).

B) *In vitro* transversal relaxivity.

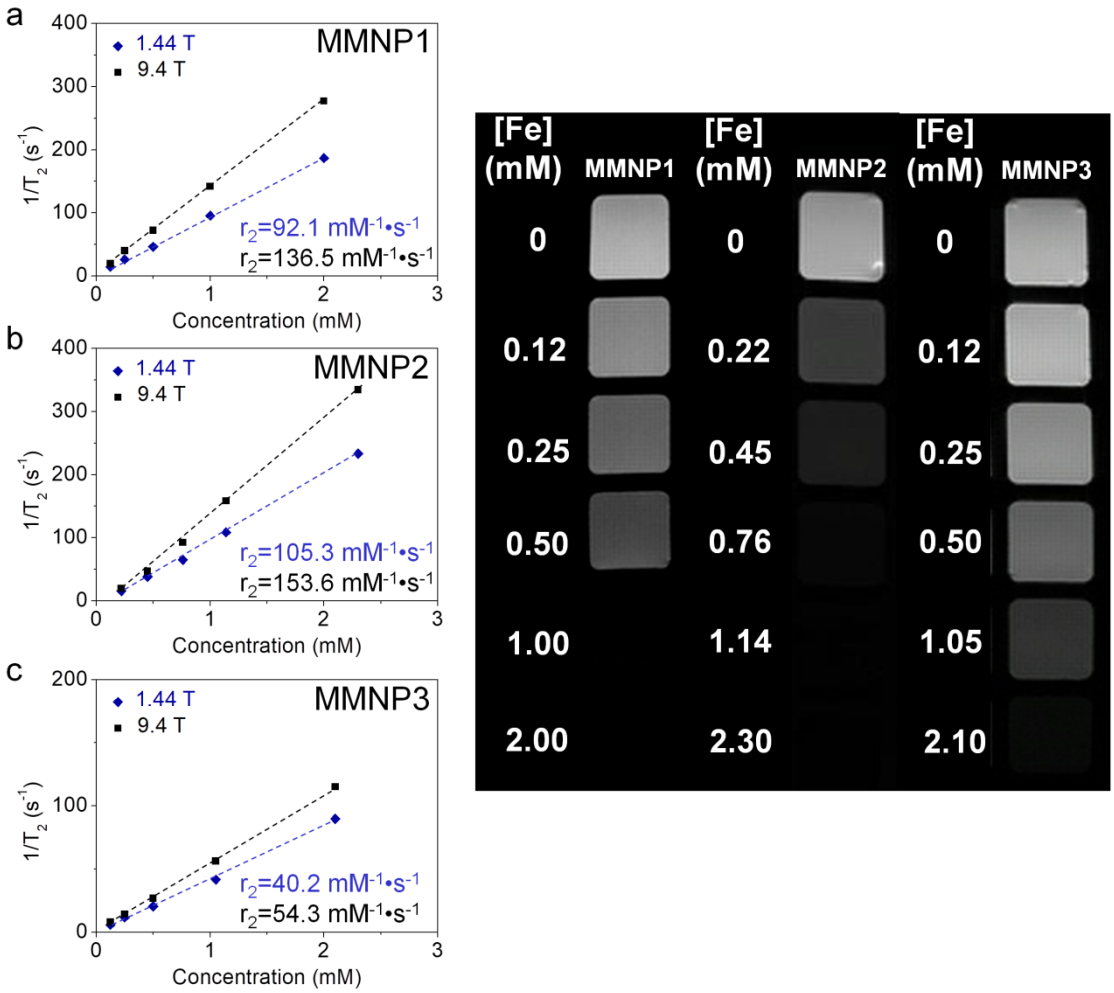

Figure S3. Plots of $1/T_2$ over Fe concentration of MMNP1 (a), MMNP2 (b), and MMNP3 (c) at 1.44 T and 9.4 T. e) T_2 weighted MR image at different concentrations of MMNPs measured at 9.4 T.

C) Cytotoxicity assays

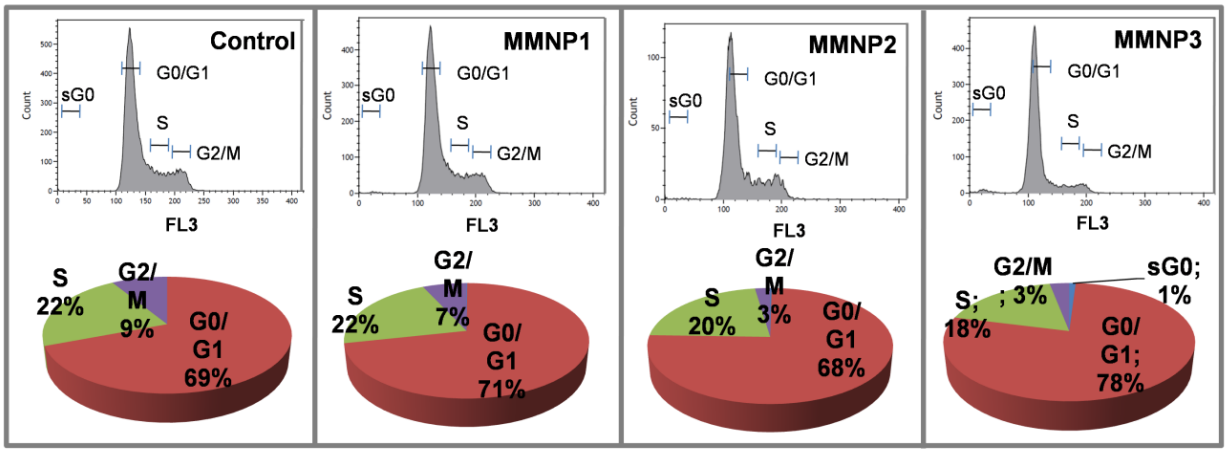

Figure S4. Flow cytometry analysis of cell cycle after 24 h of treatment with MMNP1, MMNP2, and MMNP3.

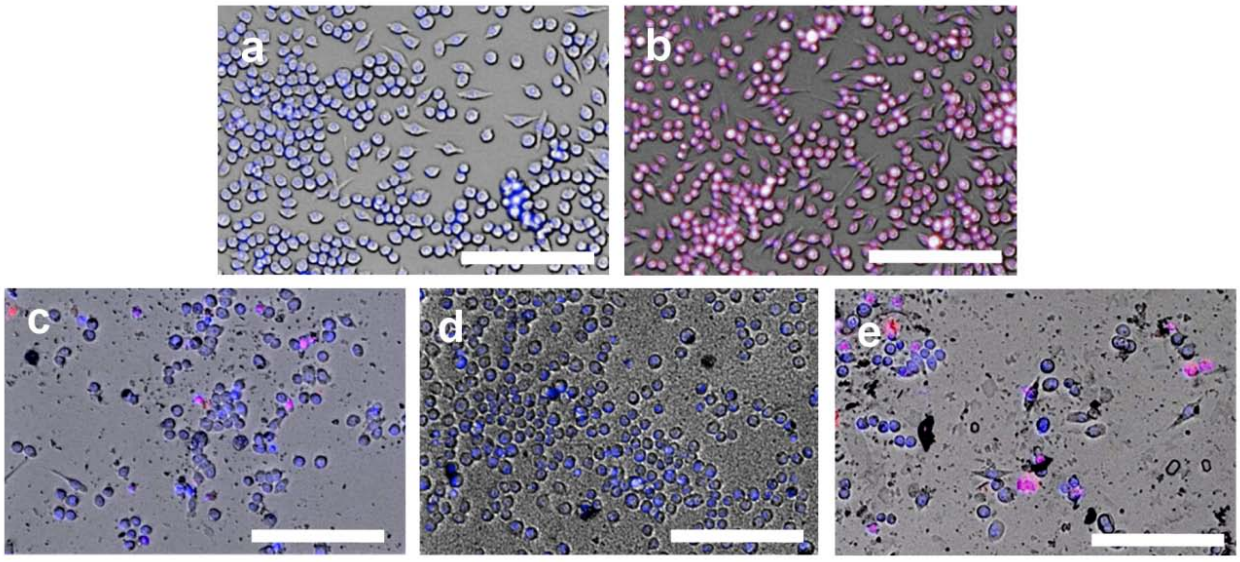

Figure S5. Images of the cultured cell exposed to different concentration of MMNPs: A) Negative control, B) Positive control, C) MMNP1 100 μg/mL, D) MMNP2 100 μg/mL, E) MMNP3 100 μg/mL. The images show the merge of brightfield (grey), DAPI (blue), and TO-PRO-3 Iodine (red).

D) *In vivo* toxicity

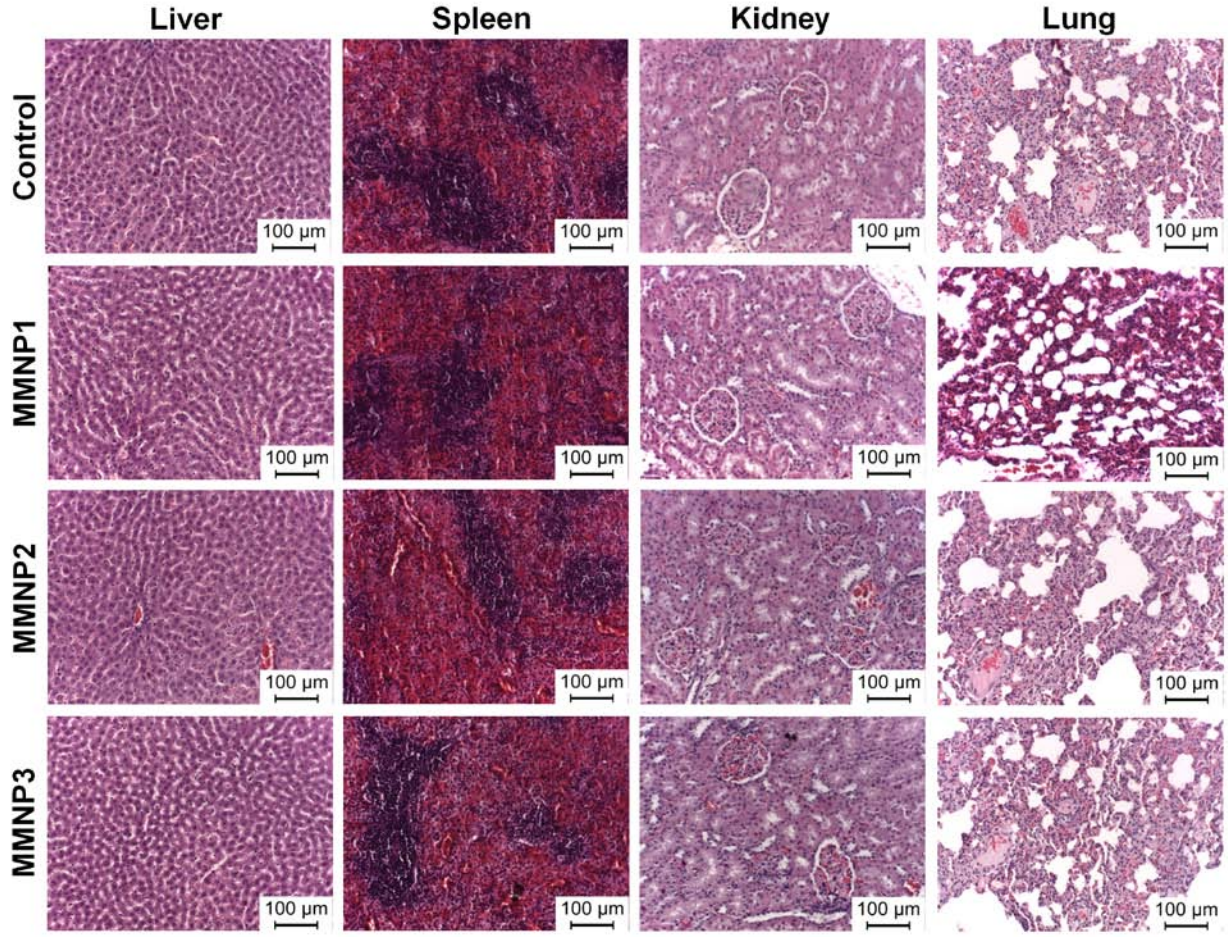

Figure S6. Representative H&E-stained histological sections of liver, spleen, kidney, and lung from tumor-bearing rats at 24 h after the intravenous administration of PBS (control) or MMNPs.

(1) Pernia Leal, M.; Rivera-Fernández, S.; Franco, J. M.; Pozo, D.; de la Fuente, J. M.; García-Martín, M. L. Long-circulating PEGylated manganese ferrite nanoparticles for MRI-based molecular imaging. *Nanoscale* **2015,** *7* (5), 2050-9.
(2) Pernia Leal, M.; Caro, C.; Garcia-Martin, M. L. Shedding light on zwitterionic magnetic nanoparticles: limitations for in vivo applications. *Nanoscale* **2017,** *9* (24), 8176-8184.